University of Glasgow
DEPARTMENT OF
AEROSPACE
ENGINEERING

A Comparative Study of Two Upwind Schemes as Applied to Navier-Stokes Solutions for Resolving Boundary Layers in Hypersonic Viscous Flow

N. QIN

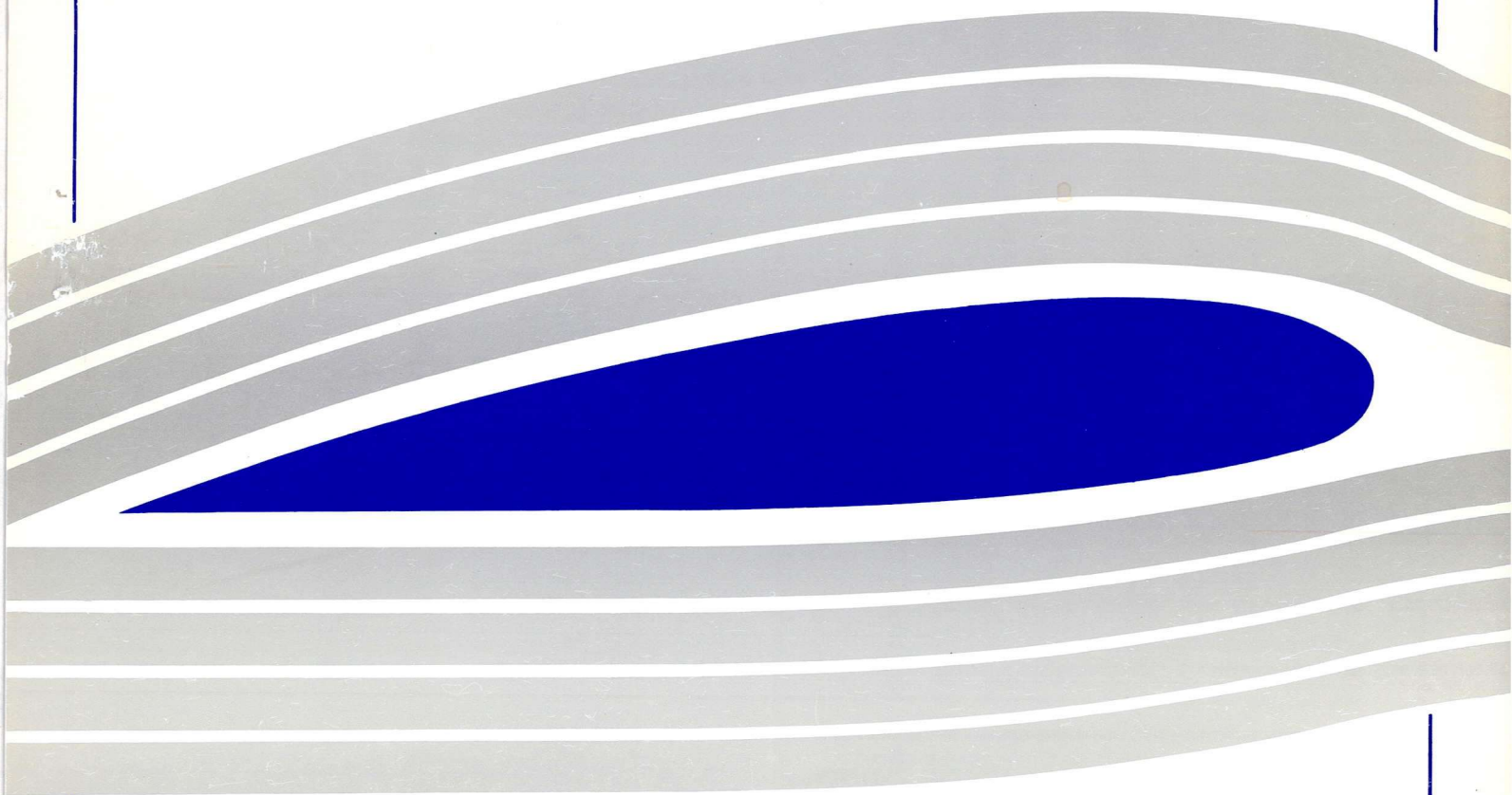

A Comparative Study of Two Upwind Schemes as Applied to Navier-Stokes Solutions for Resolving Boundary Layers in Hypersonic Viscous Flow

N. QIN

G.U. Aero. Report 9120

Department of Aerospace Engineering
University of Glasgow
Glasgow G12 8QQ

A report based on invited presentation at "Accuracy in Numerical Modelling in Computational Fluid Dynamics"
Abingdon, Oxfordshire, November 1990

June 1992

A Comparative Study of Two Upwind Schemes as Applied to Navier-Stokes Solutions for Resolving Boundary Layers in Hypersonic Viscous Flow

N. Qin

Department of Aerospace Engineering, University of Glasgow

Abstract

Van Leer's flux vector splitting scheme and Osher's flux difference splitting scheme are compared for solving the Navier-Stokes equations governing the hypersonic viscous flow. The effects of the grid number, the grid stretching, and the strength of the limiter on the solution are studied for both of the schemes. Sensitivity of the results to these parameters are then compared for the two schemes.

1. INTRODUCTION

To solve a physical problem, an appropriate mathematical model has to be set up. The accuracy of a numerical solution to the mathematical model, which is quite often a system of partial differential equations, depends mainly on the following two aspects:- (1) the numerical discretization scheme used; (2) the grid used for the discretization. In this paper we study the accuracy of the numerical solution of hypersonic viscous flows from these two aspects. The existence of both strong shock waves and thin shear layers in such a flow provides a severe test for the numerical schemes.

In the last ten to twenty years, tremendous progress have been made in devising upwind schemes for shock wave resolution for the solution of potential or Euler equations for the inviscid flow. Among these schemes are Beam and Warming's flux vector splitting, van Leer's flux vector splitting, Harten and Yee's TVD, Osher's flux difference splitting and Roe's flux difference splitting. With the development of the computer power and fast convergence numerical tools, these upwind schemes are now also being applied to the Navier-Stokes solution. They have shown the excellent capability in capturing the shock waves but their capability in resolving the viscous shear layers are quite uncertain and can be very different as shown by van Leer *et al.*[1], who showed that it is important for the numerical convective flux formula to include information about all different waves by which neighbouring cells interacts.

Two of the outstanding upwind schemes which satisfy these requirement are Roe's and Osher's flux differencing schemes. Numerical experiments for a hypersonic flow around a cone at zero angle of attack were carried out for van Leer's FVS, Roe's FDS and MacCormack's CD schemes to support this statement. However for hypersonic flows, Roe's FDS scheme in its basic form experienced problems at staganation points which are often fixed by adding some damping terms. But this 'quick fix' negated the main advantages of the scheme as pointed out by von Lavante[2]. To investigate the other outstanding upwind scheme, the Osher FDS scheme, Qin, Scriba and Richards[3] compared van Leer's FVS, Osher's FDS and MacCormack's CD schemes for a more complicated hypersonic corner flow, where Osher's FDS scheme demonstrated superior capability in capturing both the strong shock waves and the the thin shear layers as compared to the other two schemes. This motivated the present more extensive study of the schemes with a simpler flow model on the grid convergence of the solution, the sensitivity of the solution to the grid number, grid stretch and limiter strength.

2. THE GOVERNING EQUATIONS

For an extensive study of the numerical schemes, a very simple case is to be chosen. We will study the hypersonic laminar flow around a cone at zero angle of attack. For this flow, we can make two assumptions: first, the flow is axisymmetric and, therefore, the derivatives of the flow properties in the circumferential direction is zero; second, the flow is locally conical and, therefore, the derivatives of the flow properties in the conical direction is much smaller as compared to those in the crossflow surface so that they can be neglected. The locally conical Navier-Stokes equations for axisymmetric flows can be derived as follows.

Firstly, the axisymmetric Navier-Stokes Equations in general coordinate system can be written as

$$\frac{\partial \overline{\mathbf{Q}}}{\partial t} + \frac{\partial \overline{\mathbf{E}}}{\partial \xi} + \frac{\partial \overline{\mathbf{F}}}{\partial \eta} + \overline{\mathbf{H}} = 0 \tag{1}$$

where

$$\overline{\mathbf{Q}} = \mathbf{Q}/J$$
$$\mathbf{Q} = [\, \rho,\ \rho u, \rho v,\ E_t \,]^T$$

$$\overline{\mathbf{E}} = \overline{\mathbf{E}}_i - \overline{\mathbf{E}}_v$$
$$\overline{\mathbf{F}} = \overline{\mathbf{F}}_i - \overline{\mathbf{F}}_v$$

$$\overline{\mathbf{E}}_i = (\xi_x/J)\mathbf{E}_i + (\xi_y/J)\mathbf{F}_i$$
$$\overline{\mathbf{F}}_i = (\eta_x/J)\mathbf{E}_i + (\eta_y/J)\mathbf{F}_i$$

$$\overline{\mathbf{E}}_v = (\xi_x/J)\mathbf{E}_v + (\xi_y/J)\mathbf{F}_v$$
$$\overline{\mathbf{F}}_v = (\eta_x/J)\mathbf{E}_v + (\eta_y/J)\mathbf{F}_v$$

$$\mathbf{E}_i = [\, \rho u,\ \rho u^2 + p,\ \rho uv,\ (E_t + p)u \,]^T$$
$$\mathbf{F}_i = [\, \rho v,\ \rho uv,\ \rho v^2 + p,\ (E_t + p)v \,]^T$$

$$\mathbf{E}_v = [\, 0,\ \tau_{xx},\ \tau_{xy},\ u\tau_{xx} + v\tau_{xy} - q_x]^T$$
$$\mathbf{F}_v = [\, 0,\ \tau_{xy},\ \tau_{yy},\ u\tau_{xy} + v\tau_{yy} - q_y]^T$$

$$\overline{\mathbf{H}} = \overline{\mathbf{H}}_i - \overline{\mathbf{H}}_v$$

$$\overline{\mathbf{H}}_i = (v/Jy)\,[\,\rho,\ \rho u, \rho v,\ E_t + p]^T$$
$$\overline{\mathbf{H}}_v = (1/Jy)\,[\,0,\ \tau_{xy},\ \tau_{yy} - \tau_{\theta\theta},\ u\tau_{xy} + v\tau_{yy} - q_y]^T$$

where (x, y) are the Cartesian coordinates, (ξ, η) are the transformed coordinates and J is the Jacobian of the transformation, and the (x, y), (u, v), ρ, T, μ, p and E_t are non-dimensionalised using L, V_∞, ρ_∞, T_∞, μ_∞, $\rho_\infty V_\infty^2$ and $\rho_\infty V_\infty^2$, respectively. The stress tensor and the heat transfer are given as

$$\tau_{xx} = \frac{2}{3}\frac{\mu}{\mathrm{Re}}\left[2\left(\xi_x\frac{\partial u}{\partial \xi} + \eta_x\frac{\partial u}{\partial \eta}\right) - \left(\xi_y\frac{\partial v}{\partial \xi} + \eta_y\frac{\partial v}{\partial \eta}\right) - \frac{v}{y}\right]$$

$$\tau_{xy} = \frac{\mu}{\mathrm{Re}}\left(\xi_y\frac{\partial u}{\partial \xi} + \eta_y\frac{\partial u}{\partial \eta} + \xi_x\frac{\partial v}{\partial \xi} + \eta_x\frac{\partial v}{\partial \eta}\right)$$

$$\tau_{yy} = \frac{2}{3}\frac{\mu}{\mathrm{Re}}\left[2\left(\xi_y\frac{\partial v}{\partial \xi} + \eta_y\frac{\partial v}{\partial \eta}\right) - \left(\xi_x\frac{\partial u}{\partial \xi} + \eta_x\frac{\partial u}{\partial \eta}\right) + \frac{v}{y}\right]$$

$$\tau_{\theta\theta} = \frac{2}{3}\frac{\mu}{\mathrm{Re}}\left(-2\frac{v}{y} + \xi_x\frac{\partial u}{\partial \xi} + \eta_x\frac{\partial u}{\partial \eta} + \xi_y\frac{\partial v}{\partial \xi} + \eta_y\frac{\partial v}{\partial \eta}\right)$$

$$q_x = -\frac{1}{\gamma - 1}\frac{\mu}{M_\infty^2 \mathrm{RePr}}\left(\xi_x\frac{\partial T}{\partial \xi} + \eta_x\frac{\partial T}{\partial \eta}\right)$$

$$q_y = -\frac{1}{\gamma - 1}\frac{\mu}{M_\infty^2 \mathrm{RePr}}\left(\xi_y\frac{\partial T}{\partial \xi} + \eta_y\frac{\partial T}{\partial \eta}\right)$$

Applying the polar transformation

$$x = r\cos\theta$$
$$y = r\sin\theta$$

and

$$\xi = r$$
$$\eta = \eta(\theta)$$

to the above equation we then have the locally conical Navier-Stokes equations for axisymmetric flows as follows

$$\frac{\partial \overline{\mathbf{Q}}}{\partial t} + \frac{\partial \overline{\mathbf{F}}}{\partial \eta} + \widehat{\mathbf{H}} = 0 \qquad (2)$$

$$\widehat{\mathbf{H}} = \overline{\mathbf{H}} + \overline{\mathbf{E}}/\xi$$

The derivatives of the velocity components and the temperature with respect to ξ are also neglected in the stress tensor and heat transfer terms.

To relate the state variables, we have

$$p = (\gamma - 1) [E_t - \frac{1}{2} \rho (u^2 + v^2 + w^2)] \tag{3}$$

$$T = \gamma M_\infty^2 p / \rho \tag{4}$$

and the viscosity is calculated from temperature T through the Sutherland formula.

3. THE NUMERICAL SCHEMES

For the viscous terms in the governing equations, a central difference scheme is used. The key issue is the choice of numerical schemes in the discretization of convective fluxes. Studied here are the two schemes for spatial discretization of the convective fluxes: (1) Van Leer's flux vector splitting scheme(FVS); and (2) Osher's flux difference splitting scheme(FDS).

3.1. Inviscid Fluxes Evaluation

In the cell centred finite difference formulation employed here, the state variables $\mathbf{Q}$ are evaluated at cell centres and represent cell-averaged values. The flux $\overline{\mathbf{F}}_i$ is evaluated at cell interfaces. The spatial derivatives are then represented as a flux balance across a cell. The interface flux is determined from a local one-dimensional model of wave interactions normal to the cell interfaces. Using the flux vector splitting (FVS) model developed by van Leer[4], the interface flux can be written as

$$\widetilde{\mathbf{F}}_i = \overline{\mathbf{F}}_i^{+}(\mathbf{Q}^L) + \overline{\mathbf{F}}_i^{-}(\mathbf{Q}^R) \tag{5}$$

where $\overline{\mathbf{F}}_i^{+}$ and $\overline{\mathbf{F}}_i^{-}$ denote positive and negative split flux contributions and $\mathbf{Q}^L$ and $\mathbf{Q}^R$ denote state variables on either side of the interface.

With the flux difference splitting (FDS) model developed by Osher *et al.*[5,6], the interface flux can be written as

$$\widetilde{\mathbf{F}}_i = \frac{1}{2}\left[\, \overline{\mathbf{F}}_i(\mathbf{Q}^L) + \overline{\mathbf{F}}_i(\mathbf{Q}^R) - \int_{\mathbf{Q}^L}^{\mathbf{Q}^R} \left|\frac{\partial \overline{\mathbf{F}}_i}{\partial \mathbf{Q}}\right| d\mathbf{Q} \,\right] \tag{6}$$

where the integral in the state variable domain is carried out along a path piecewise parallel to the eigenvectors of $\partial\overline{\mathbf{F}}_i/\partial\mathbf{Q}$. Osher *et al.*[5-6] proposed a reverse ordering of the subcurves while a natural ordering, which needs less flux calculations, has been employed here according to Spekreijse[7] in calculating the integral in the above interface flux. This technique reduces considerably the computation normally associated with the Osher scheme.

3.2 The MUSCL Scheme for High Order Accuracy and the Limiter

The state-variable interpolations determine the resulting accuracy of the scheme. It was found in the present research that the use of primitive variables $\mathbf{q} = [\,\rho, u, v, p\,]^T$ in the interpolation is more robust than the use of conserved variables $\mathbf{Q}$ in the sense that non-physical states from the interpolation, such as, negative pressure, are easier to avoid. A κ-parameter family of higher-order schemes[8] can be written as

$$\begin{aligned} \mathbf{q}^{L}_{i+\frac{1}{2}} &= \mathbf{q}_i + \{(\tfrac{s}{4})[(1-\kappa s)\Delta_- + (1+\kappa s)\Delta_+]\mathbf{q}\}_i \\ \mathbf{q}^{R}_{i+\frac{1}{2}} &= \mathbf{q}_{i+1} - \{(\tfrac{s}{4})[(1+\kappa s)\Delta_- + (1-\kappa s)\Delta_+]\mathbf{q}\}_{i+1} \end{aligned} \tag{7}$$

where Δ_+ and Δ_- denote forward and backward difference operators, respectively, in the η direction. The parameter κ determines the spatial accuracy of the difference approximation: $\kappa = -1$ corresponds to a fully-upwind second order scheme, $\kappa = 1$ to a central difference scheme, and $\kappa = 1/3$ to a third order upwind-biased scheme. In the following calculation, $\kappa = 1/3$ is chosen for nominal higher order of accuracy to avoid unnecessary numerical dissipation introduced from a nominal lower order scheme.

The parameter s serves to limit higher-order terms in the interpolation in order to avoid oscillations at discontinuities such as shock waves in the solutions. According to Anderson *et al.*[9], the limiting is implemented by locally modifying the difference values in the interpolation to ensure monotone interpolation as

$$s = \frac{2\Delta_+\mathbf{q}\Delta_-\mathbf{q} + \varepsilon}{(\Delta_+\mathbf{q})^2 + (\Delta_-\mathbf{q})^2 + \varepsilon} \tag{8}$$

where ε is a small number preventing division by zero in regions of null gradients.

3.3. Time Dependent Approach for Steady State Solution

Time dependent approaches were used to solve the problem for a steady state solution. For the above two upwind schemes, a 4-stage Runge-Kutta scheme was used for the time discretization. Local time stepping has been used to improve the convergence. The common feature of the two upwind schemes is their continuous differentiability, which guarantees the applicability of a Newton type solution technique for fast convergence of the solution[10].

4. RESULTS

The geometry and the flow conditions are based on the experimental work of Tracy[11]. The geometry is a sharp cone with a half cone angle of 7°. The incoming flow is at a Mach number of 7.95, a Reynolds number of 4.1×10^6/meter and a temperature of 55.4 K. The wall is a isothermal wall at a temperature of 309.8 K.

4.1 Grid and Boundary Conditions

The computation is carried out at station $\xi = 0.09$ and the grid in η direction is generated using Robert's boundary layer stretching transformation[12], which can be written as

$$\theta_1 = \theta_c, \quad \theta_I = \theta_{max}$$

$$\theta_i = \theta_1 + (\theta_I - \theta_1)\frac{(\beta+1)-(\beta-1)\left(\frac{\beta+1}{\beta-1}\right)^{1-\frac{i-1}{I-1}}}{\left(\frac{\beta+1}{\beta-1}\right)^{1-\frac{i-1}{I-1}}+1} \quad (1<\beta<\infty)$$

With the above transformation from the physical domain to the computational domain, the points in the physical domain will be clustered toward the wall, which is controlled by the stretching factor β. The closer the factor β is to unit, the more points will be clustered near the wall.

The boundary conditions are set up as following. At the wall, a non-slip and isothermal wall boundary condition is applied. At the outer boundary, which is outside the shock wave, the flow is fixed to the incoming flow condition.

4.2 Convergence of the Solution to the Grid

Grid convergent results were obtained by doubling the grid number but with a fixed stretching factor until the results no longer changes with a denser grid. In Fig.1 we plot out the reasonably converged results of temperature profiles for both schemes. They are obtained on a 65 points grid with stretch factor of 1.01. As can be seen in the following sections, the convergence of the solution to the grid is quite different for the two different schemes. It should be noted that Osher's FDS results is in fact converge on a much coarser grid. The converged results from the two schemes are shown to be in very good agreement. These converged profiles are used in the following sections as a standard for the study of sensitivity of the schemes to different grid and numerical parameters.

4.3 Sensitivity of the Solution to the Grid Number

Sensitivity of the solution to the grid number were studied by comparing the results on successively coarser grid with the grid converged results. Temperature profiles are shown in Figs. 2,3 for solutions using different grid numbers, namely, 9, 17, 33 or 65 grid points in the θ direction in the flowfield. Results in Fig. 2 were obtained from the Osher FDS scheme and in Fig. 3 from the van Leer FVS scheme. The solid lines represent grid converged results.

It is shown from these profiles that the results from the Osher FDS scheme are much less sensitive than the van Leer FVS scheme. Especially in the boundary layer, the results of the Osher FDS scheme captured the shear layer with as few as 8 grid points while those of the van Leer FVS scheme are still further away from the converged results with 15 points in the boundary layer.

Another observation from the results of the van Leer FVS scheme is that better resolution of the boundary layer using this scheme can be obtained by using denser grid in the whole boundary layer region.

4.4 Sensitivity of the Solution to the Grid Stretch

Grid for Navier-Stokes solutions are usually clustered towards the wall to satisfy the requirement for the resolution of boundary layers. One widely used way to achieve this is by using a stretch formula in generating the grid in the wall normal direction. Figs. 4,5 show the results obtained by the two schemes using different stretching factor but a fixed grid number.

For the Osher FDS scheme, the results are not sensitive to the different stretching of the grid. As the boundary layer can be captured with only 7-8 grid points, high clustering of the grid near the wall seems not to be beneficial for the sake of better shock wave resolution in the inviscid flow region.

On the other hand, for the van Leer FVS scheme, the results varies with the stretch factor in a complicated way. Higher stretch distributes more grid points in the boundary layer. But to capture the boundary layer as a whole, further stretch seems not to be a good idea because the wall shear layer will get unnecessarily too many grid points while the shear layer up the wall will still be lack of grid points.

4.5 Sensitivity of the Solution to the Limiter Strength

The strength of the limiter in Eq.(8) is controlled by the parameter ε, which was originally only used to prevent division by zero in regions of null gradients. With the increase of the parameter ε the strength of the limiter reduces. If ε is so larger that it becomes dominant terms as compared to the difference terms in the formula, the limiter will actually be switched off.

Figs. 6,7 show the results for different limiter strength with a fixed grid number and a fixed grid stretch factor. For both schemes, the results indicate that the boundary layer resolution is not sensitive to this parameter except that the overshoot at the shock wave start to appear for the largest ε. No improvement can be observed for the boundary layer resolution with the FVS scheme by reducing the influence of the limiter.

5. CONCLUDING REMARKS

From the present study, we may draw the following conclusions:

(1) Boundary layer resolution for Navier-Stokes solution is very sensitive to the numerical discretization scheme chosen. They are more important than other aspects which influence the accuracy of the solution such as the grid density, stretching factor or the strength of the limiter.

(2) The Osher FDS scheme can capture the boundary layer with a comparatively very small amount of grid points so that the solution is not sensitive to the grid, neither the grid number nor the grid stretch factor.

(3) The van Leer FVS scheme, when applied to Navier-Stokes solution, capture the boundary layer poorly and, therefore, many more grid points are required to resolve the shear layers in the boundary layer, which results in the sensitivity of the solution to the grid, both the grid number and the stretch factor.

(4) The boundary layer results produced by both schemes are not sensitive to the limiter strength. One future work is to test the sensitivity of the solution when different types of limiters are used.

ACKNOWLEDGEMENTS

The author sincerely thanks Prof. Bryan Richards for his continuous encouragement and useful advices during the present research. He gratefully acknowledges the support by B.Ae. Dynamics under Contract GF376605 monitored by Dr. Richard Tod.

REFERENCES:

1. Van Leer, B., Thomas J. L., Roe P. and Newsome R. W., "A Comparison of Numerical Flux Formulas for the Euler and Navier-Stokes Equations," AIAA Paper 87-1104, June 1987.

2. Von Lavante, E., "Accuracy of Upwind Schemes Applied to the Navier-Stokes Equations,"
AIAA J., Vol. 28, No. 7, July 1990, pp 1312-1314.

3. Qin, N., Scriba, K.W. and Richards, B.E., "Shock-shock, Shock-Vortex Interaction and Aerodynamic Heating in Hypersonic Corner Flow"
The Aeronautical Journal, Vol. 95, No. 945, May 1991, pp152-160.

4. Van Leer, B., "Flux Vector Splitting for the Euler Equations,"
Lect. Notes in Phys. Vol. 170, 1982, pp507-511.

5. Osher, S. and Solomon, F., "Upwind Schemes for Hyperbolic Systems of Conservation Laws",
Math. Comp., Vol.38, 1982, pp339-374.

6. Osher, S. and Chakravarthy, S. R., "Upwind Schemes and Boundary Conditions with Applications to Euler Equations in General Coordinates",
J. Comp. Phys., Vol. 50, 1983, pp447-481.

7. Spekreijse, S. P., "Multigrid Solution of the Steady Euler Equations",
Ph.D. Thesis, CWI 1987 also available as CWI Tract 46, 1988, Amsterdam.

8. Van Leer, B., "Upwind-Difference Methods for Aerodynamic Problems Governed by the Euler Equations,"
Lect in Appl Math, Vol. 22, Part II, 1985, pp327-336.

9. Anderson, W. K., Thomas, J. L. and van Leer, B., "A Comparison of Finite Volume Flux Vector Splittings for the Euler Equations",
AIAA J., Vol.24, No.9, 1986, pp1453-1460.

10. Qin, N. and Richards, B.E., "Sparse Quasi-Newton Method for Navier-Stokes Solution,"
Notes on Numerical Fluid Mechanics, Vol. 29, 1990, pp474-478.

11. Tracy, R. R., "Hypersonic Flow over a Yawed Circular Cone," California Institute of Technology Aeronautical Laboratory Memorandum, No.69, 1963.

12. Roberts, G. O., "Computational Meshes for Boundary Layer Problems," *Lect.. Notes in Phys.*, Vol.8, 1971, pp171-177.

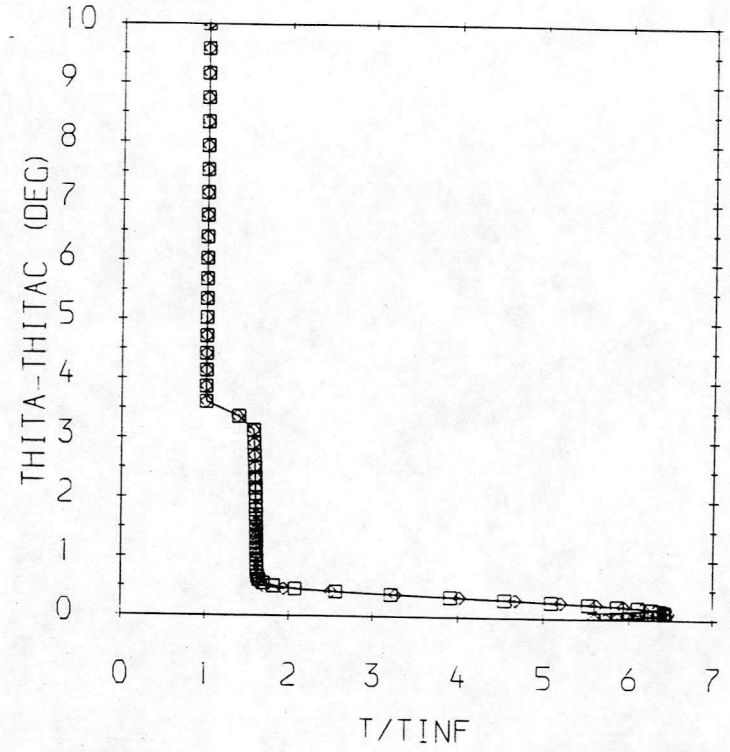

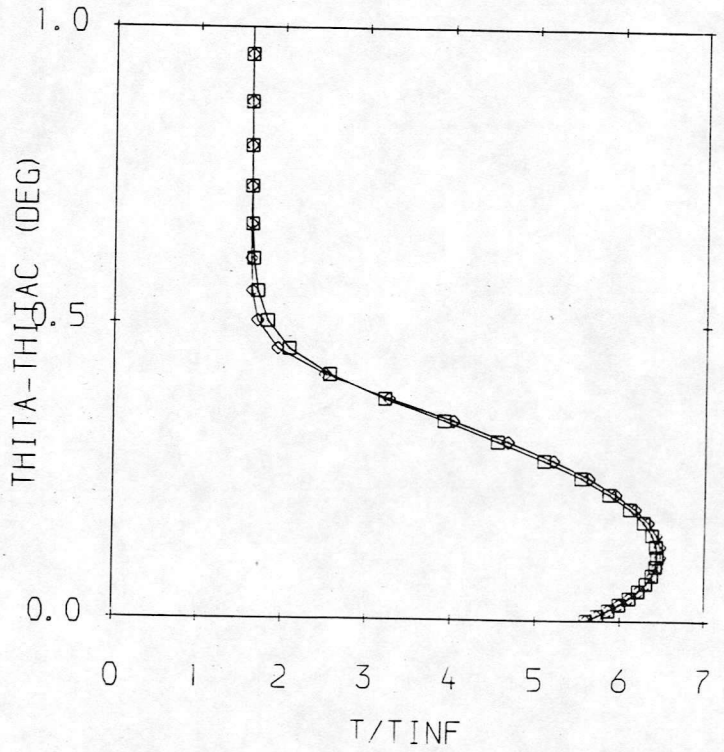

Fig. 1 Grid convergent results, 65 points, $\beta = 1.01$

⊟—⊟ FVS ⟷ FDS

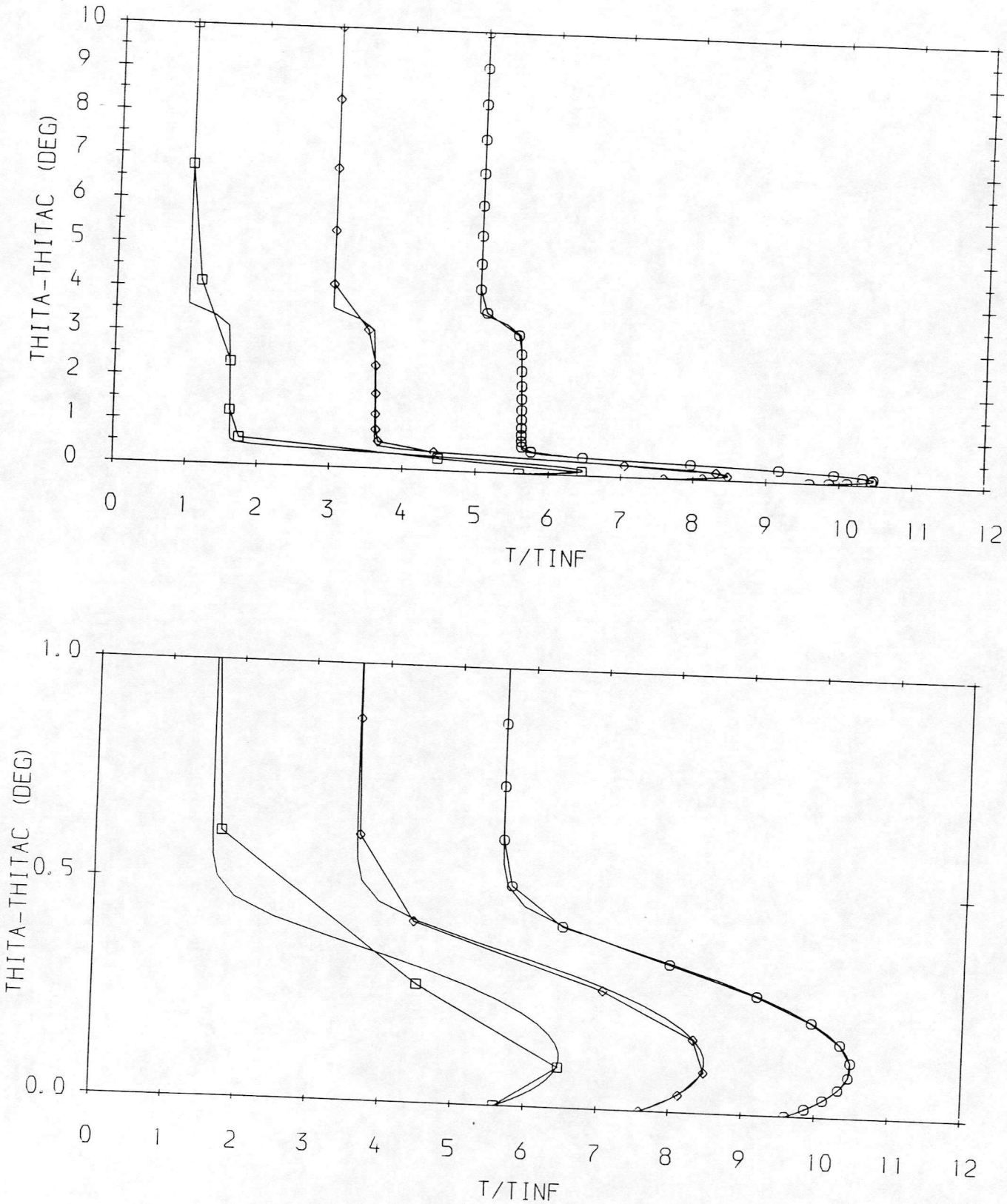

Fig. 2 Sensitivity to the grid number - Osher's FDS, $\beta = 1.01$

9 points; 17 points; 33 points

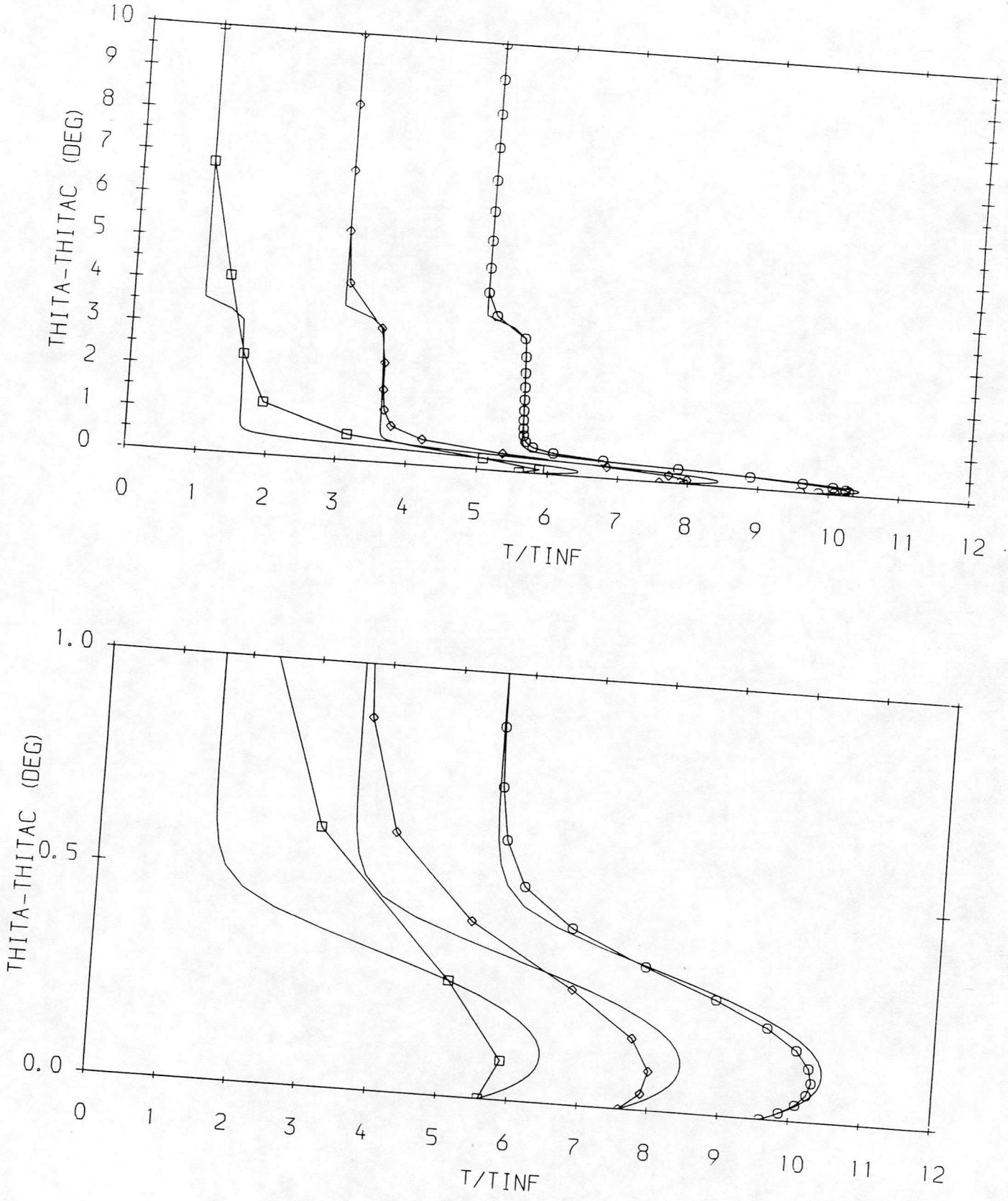

Fig. 3 Sensitivity to the grid number - van Leer's FVS, $\beta = 1.01$

9 points; 17 points; 33 points

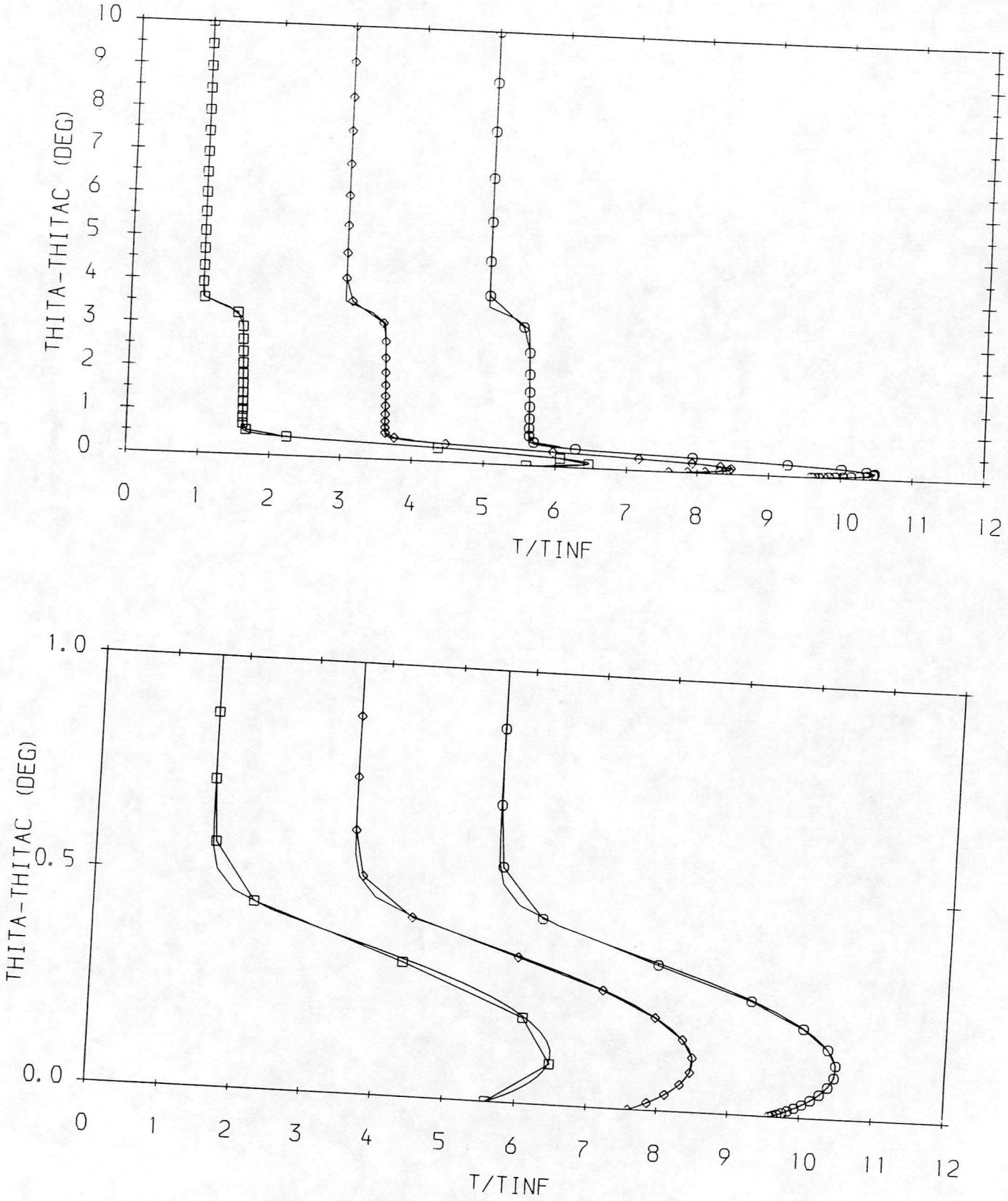

Fig. 4 Sensitivity to the stretch factor - Osher's FDS, 33 points

β= 1.1; β = 1.01; β= 1.001

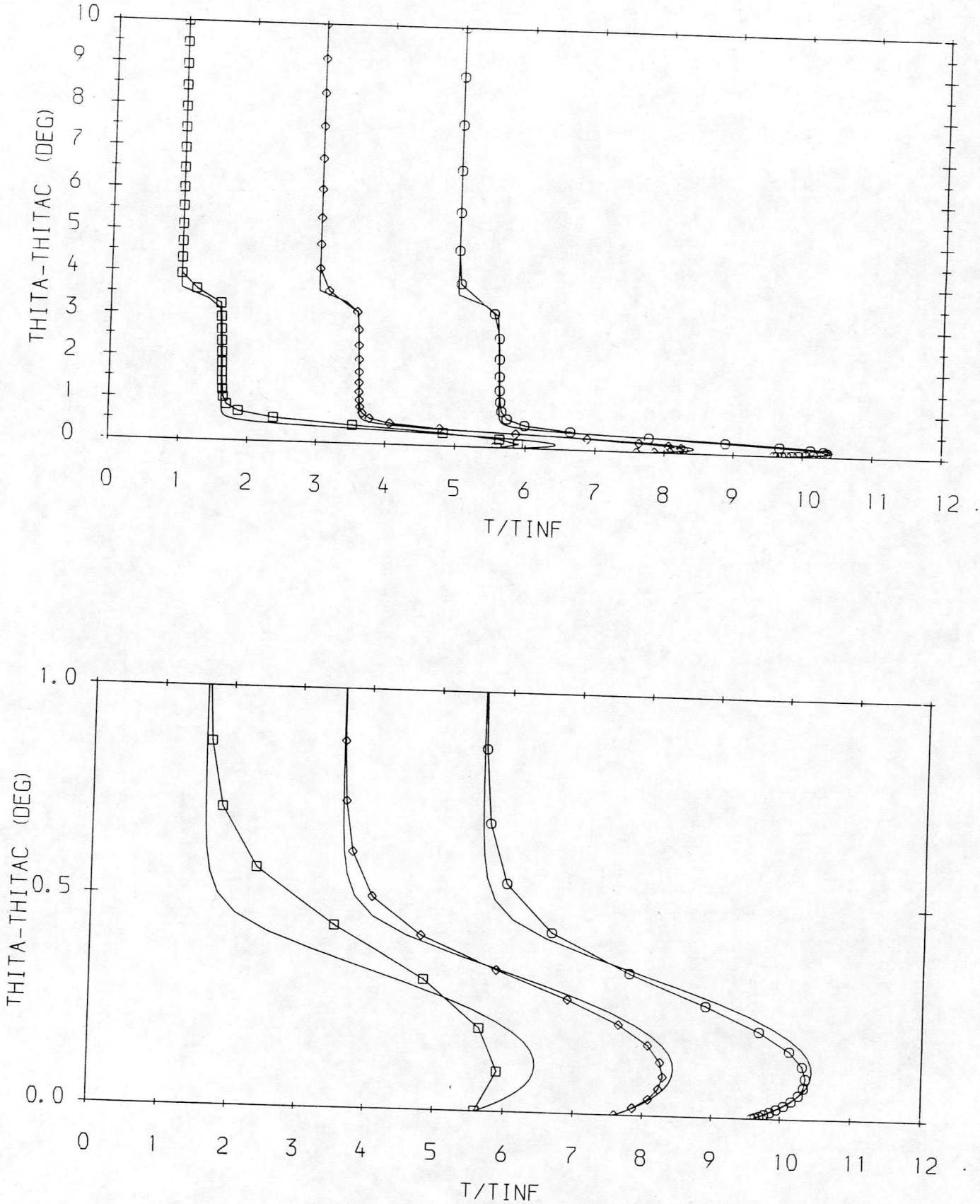

Fig. 5 Sensitivity to the stretch factor - van Leer's FVS, 33 points

$\beta = 1.1$; $\beta = 1.01$; $\beta = 1.001$

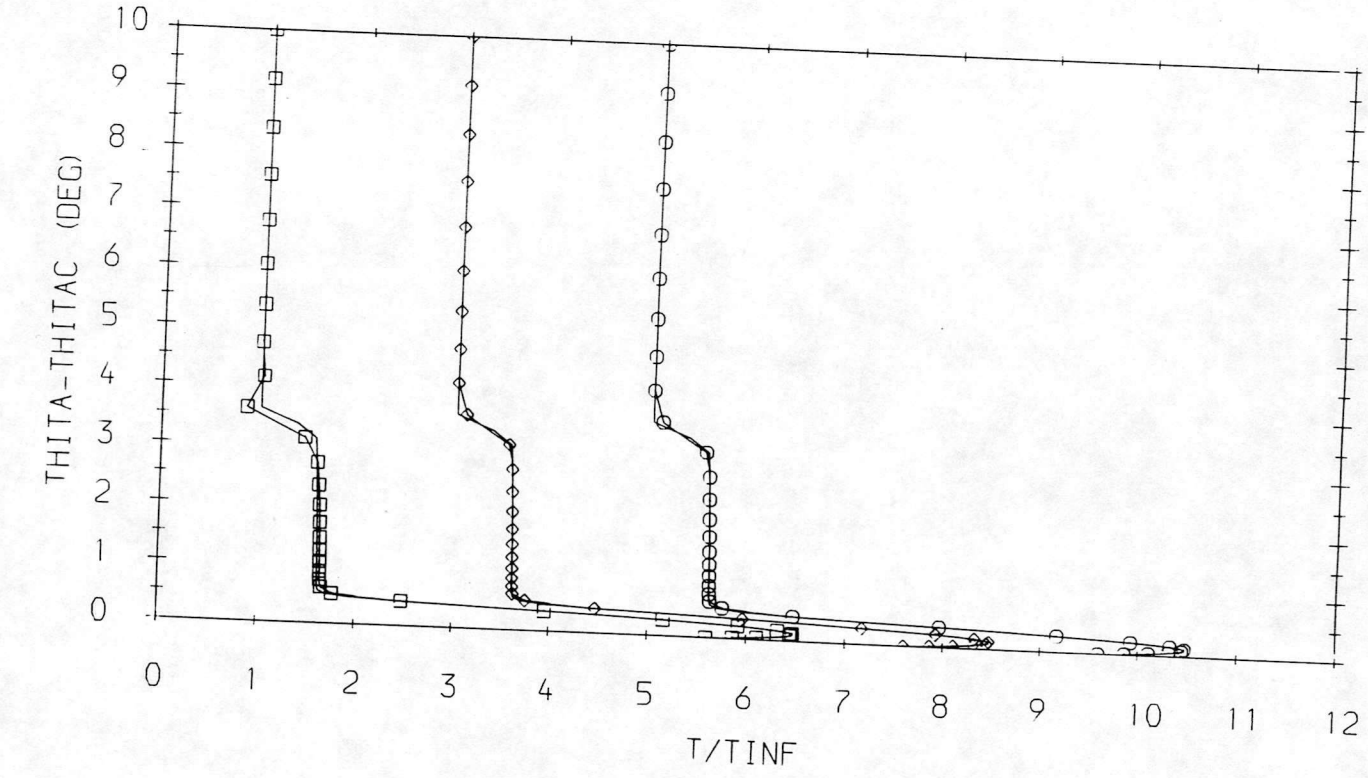

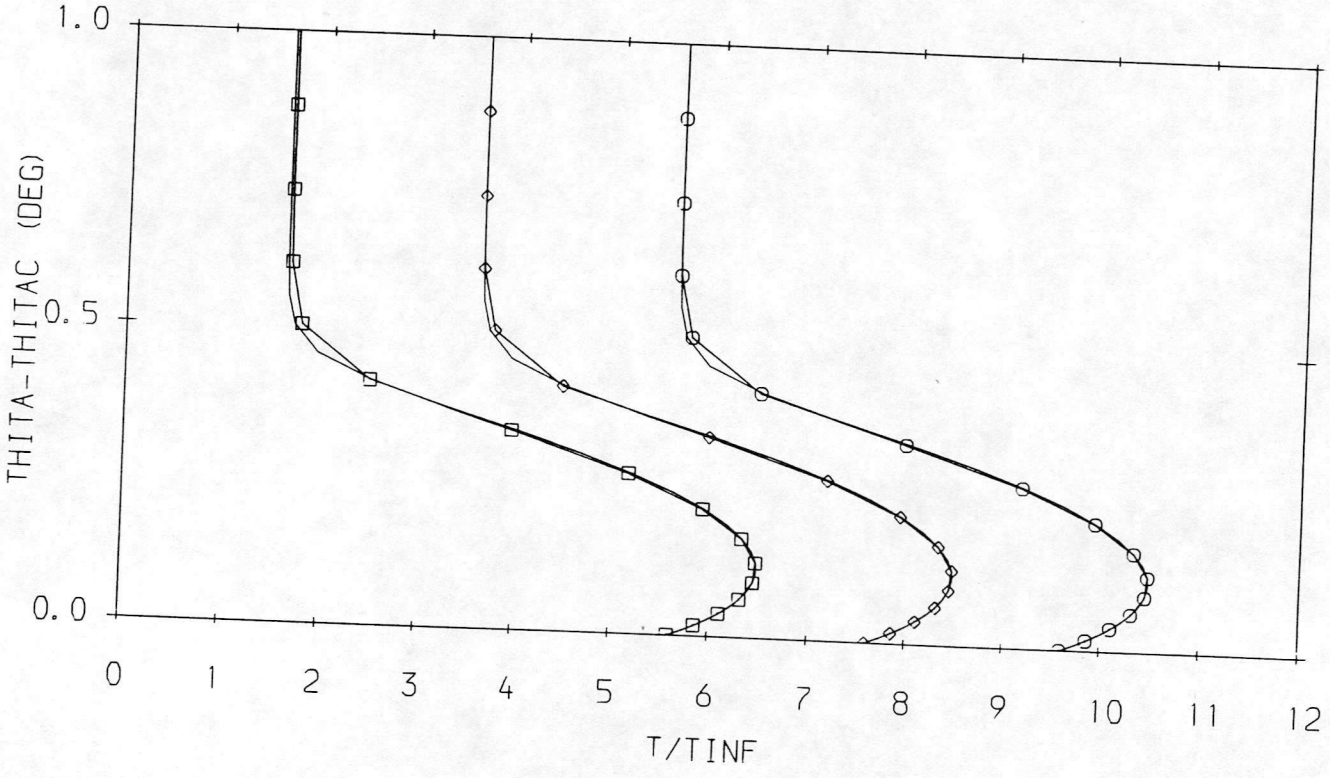

Fig. 6 Sensitivity to the limiter strength - Osher's FDS, 33 points, $\beta = 1.01$

$\varepsilon = 10^{-3}$; $\varepsilon = 10^{-7}$; $\varepsilon = 10^{-13}$

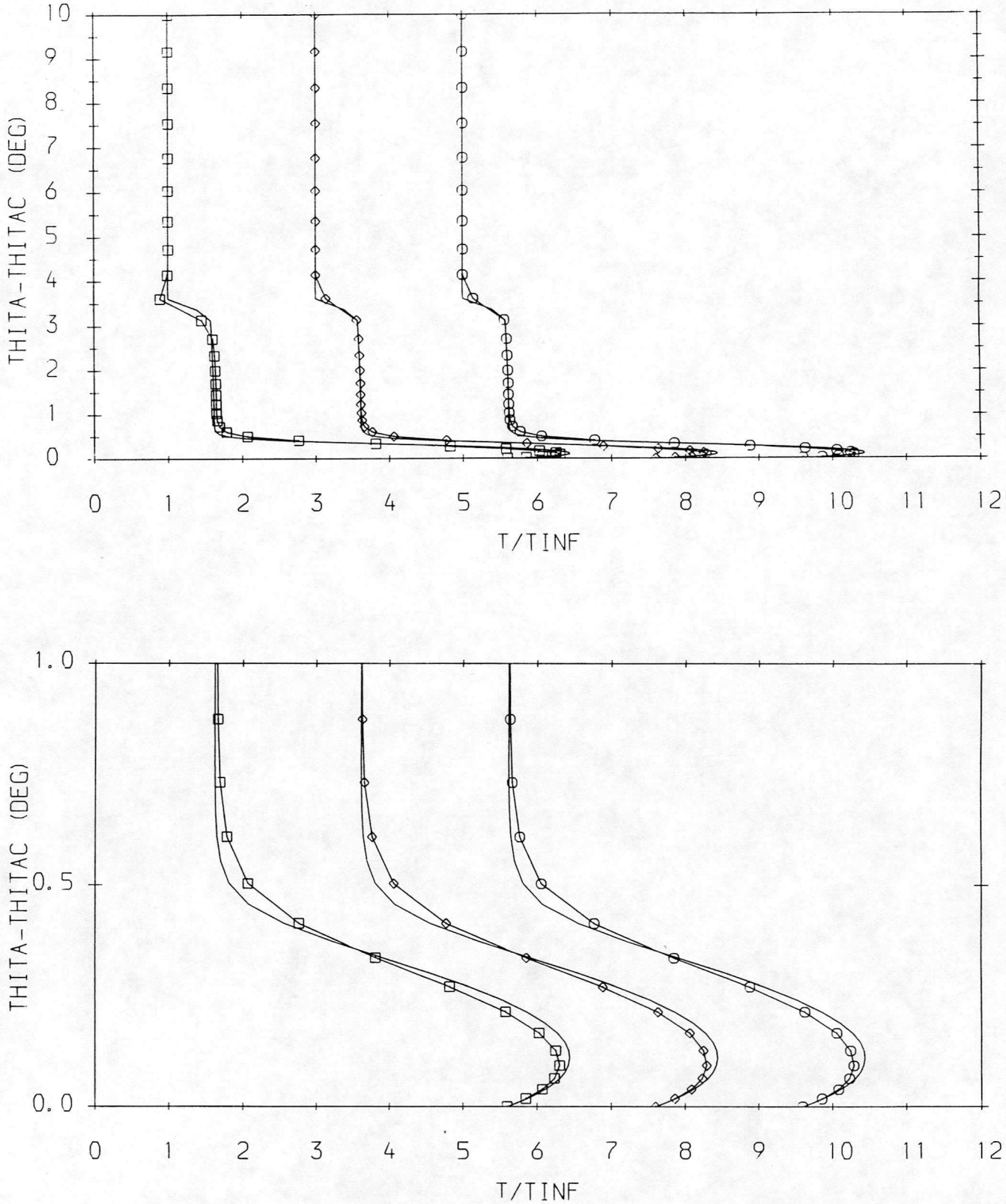

Fig. 7 Sensitivity to the limiter strength - van Leer's FVS

$\varepsilon = 10^{-3}$; $\varepsilon = 10^{-7}$; $\varepsilon = 10^{-13}$